Biofouling
Publication details, including instructions for authors and subscription information:
http://www.informaworld.com/smpp/title~content=t713454511

Influence of an oil soluble inhibitor on microbiologically influenced corrosion in a diesel transporting pipeline

N. Muthukumar [a]; S. Maruthamuthu [a]; S. Mohanan [a]; N. Palaniswamy [a]
[a] Central Electrochemical Research Institute, Karaikudi, India

First Published on: 17 September 2007

To cite this Article Muthukumar, N., Maruthamuthu, S., Mohanan, S. and Palaniswamy, N.(2007)'Influence of an oil soluble inhibitor on microbiologically influenced corrosion in a diesel transporting pipeline',Biofouling,23:6,395 — 404
To link to this Article: DOI: 10.1080/08927010701567846
URL: http://dx.doi.org/10.1080/08927010701567846

Biofouling, 2007; 23(6): 395 – 404

Taylor & Francis
Taylor & Francis Group

Influence of an oil soluble inhibitor on microbiologically influenced corrosion in a diesel transporting pipeline

N. MUTHUKUMAR, S. MARUTHAMUTHU, S. MOHANAN & N. PALANISWAMY

Central Electrochemical Research Institute, Karaikudi, India

(Received 25 December 2006; accepted 12 July 2007)

Abstract
Microbial degradation of the oil soluble corrosion inhibitor (OSCI) Baker NC 351 contributed to a decrease in inhibitor efficiency. Corrosion inhibition efficiency was studied by the rotating cage and flow loop methods. The nature of the biodegradation of the corrosion inhibitor was also analysed using Fourier transform infrared spectroscopy, nuclear magnetic resonance spectroscopy and gas chromatography-mass spectrometry. The influence of bacterial activity on the degradation of the corrosion inhibitor and its influence on corrosion of API 5LX were evaluated using a weight loss technique and impedance studies. *Serratia marcescens* ACE2 and *Bacillus cereus* ACE4 can degrade aromatic and aliphatic hydrocarbons present in the corrosion inhibitor. The present study also discusses the demerits of the oil soluble corrosion inhibitors used in petroleum product pipeline.

Keywords: *Diesel pipeline, oil soluble corrosion inhibitor (OSCI), rotating cage method, flow loop method, biodegradation, microbiologically influenced corrosion*

Introduction

The possible effects of corrosion inhibitors on bacteria are of considerable interest to those involved in oil and gas production and transmission. It is possible that corrosion inhibitors have biocidal effects on bacteria (Pope et al. 1989). Organic film-forming inhibitors used in the oil and gas industry are generally of the cationic/anionic type and include imidazolines, primary amines, diamines, amino-amines, oxyalkylated amines, fatty acids, dimer-trimer acids, naphthaneic acid, phosphate esters and dodecyl benzene sulphonic acids. Their mechanism of action is to form a persistent monolayer film adsorbed at the metal-solution interface. It is well known that bacteria can oxidise a wide variety of chemicals and use them as nutrient sources enhancing the proliferation of bacteria (Ram et al. 1982; Lin et al. 1989; Rajasekar et al. 2006). Microorganisms influence corrosion by altering the chemistry at the interface between metal and the bulk fluid (Shennan, 1988; Videla & Characklis, 1992; Bento & Gaylarde, 2001; Jones & Amy, 2002; Little & Ray, 2002. Muthukumar et al. (2003) and Bento et al. (2005) described the microbial species involved in corrosion and their interactions with metal surfaces. Maruthamuthu et al. (2005) and Rajasekar et al. (2006) reported that microbial degradation of a corrosion inhibitor during use can affect their specific performance on corrosion inhibition in petroleum product pipelines. Microbial degradation of simple heterocyclic inhibitors of the type morpholine (C_4H_9NO) had been reported by Poupin et al. (1998). Recently, the degradation of a water-soluble corrosion inhibitor was observed in a mixed diesel-water system in the presence of bacteria (Muthukumar et al. 2006). Before selection of an oil souble corrosion inhibitor (OSCI) it is essential to determine whether the inhibitor is a nutrient source or biocide. Hence, in the present study a laboratory experiment was designed to evaluate the degradation of an OSCI, using the bacterial species *Serratia marcescens* ACE2 and *Bacillus cereus* ACE4.

In oil pipelines, water can stratify at the bottom of a line if the velocity is less than that required to entrain water and sweep it through the pipeline system. Liquids stratify along the bottom of the pipe, with water forming a separate layer beneath insoluble hydrocarbons. The involvement of bacterial species on inhibitor degradation and corrosion has been studied by various investigators (Freiter 1992; Prasad 1998; Rajasekar et al. 2006).

Correspondence: N. Palaniswamy, Central Electrochemical Research Institute, Karaikudi – 630 006, India. Fax: +91 4565 227779.
E-mail: swamy23@rediffmail.com

ISSN 0892-7014 print/ISSN 1029-2454 online © 2007 Taylor & Francis
DOI: 10.1080/08927010701567846

Experimental

Background information to the study

A cross-country pipeline in India, transports petroleum products such as kerosene, petrol and diesel. This pipeline has intermittent petroleum product pressure booting stations at different locations. Severe corrosion and microfouling problems have been identified in the pipeline even though a corrosion inhibitor was added. About 200–400 kg of sediment (corrosion product) was removed from a 200 km stretch of the pipeline after 30 d of operation (Maruthamuthu et al. 2005). The corrosion product was pushed out of the pipeline by pigs (cylindrical devices that move with the flow of oil and clean the pipeline interior) while cleaning the pipeline. The corrosion product samples were collected in sterile containers for microbial enumeration and identification. In the present study, a commercially available OSCI, Baker NC 351, supplied by Baker, India, used in petroleum transporting pipelines was evaluated.

Composition of the OSCI

The OSCI, Baker NC 351, which contains amine based mono-carboxylic acid compounds, was further characterised by GC-MS. The composition of the OSCI is presented in the Results. The vendor, Baker, India, recommended 10 ppm of the OSCI for petroleum transporting pipeline. In the present study, 100 ppm of the OSCI was selected for the corrosion study and 400 ppm for the degradation study. Because of water stagnation at low velocity areas of operational pipelines (Maruthamuthu et al. 2005), these high levels of OSCI were selected for degradation and corrosion studies to stimulate field conditions.

Microorganisms

The bacteria *Serratia marcescens* ACE2 and *Bacillus cereus* ACE4 (Rajasekar et al. 2006) used in this study were isolated from an oil transporting pipeline. The nucleotide sequences for ACE2 and ACE4 have been deposited in GenBank under the sequence numbers DQ092416 and AY912105.

Composition of the growth medium

The medium used for detecting the OSCI degrading process by ACE2 and ACE4 was Bushnell–Hass (BH) broth (magnesium sulphate, 0.20 gm l^{-1}; calcium chloride, 0.02 gm l^{-1}; monopotassium phosphate, 1 gm l^{-1}; di-potassium phosphate, 1 gm l^{-1}; ammonium nitrate, 1 gm l^{-1}; ferric chloride, 0.05 gm l^{-1}, Hi-Media, Mumbai) and BH agar. Three sets of Erlenmeyer flasks were used for the inhibitor degradation studies using the selected bacterial strains.

Biodegradation and characterisation of the OSCI

Two sets of Erlenmeyer flasks containing 100 ml of BH broth, 400 ppm of OSCI with ACE2 and ACE4 were inoculated. An uninoculated control flask was incubated in parallel to monitor abiotic losses of the corrosion inhibitor. The flasks were incubated at 30°C for 30 d in an orbital shaker (150 rpm). At the end of the 30-d incubation, the residual OSCI (1 μl) was extracted with an equal volume of dichloromethane (1 μl). Evaporation of the solvent was carried out in a hot water bath at 40°C. About 1 μl of the resultant solution was analysed by Fourier transform infrared spectroscopy (FTIR) and H^1 nuclear magnetic resonance spectroscopy (NMR). FTIR spectra (Nicolet Nexus 470) were taken in the mid IR region of 400–4000 cm^{-1} with 16-scan speed. The samples were mixed with spectroscopically pure KBr in the ratio of 1:100 and the pellets were fixed in the sample holder. Infrared peaks localised at 2960 and 2925 cm^{-1} were used to calculate the CH_2/CH_3 ratio (absorbance) and functional group of both aliphatic and aromatic components present in OSCI. H^1 NMR (Bruker, 400 mHz) analysis was used to detect the protons of the nuclei in the diesel compound. The sample of diesel was dissolved using deutrated chloroform solvent. Tetramethyl silane (TMS) was used as a reference standard. The 1 μl of the resultant corrosion inhibitor solution was analysed by Thermo Finnigan gas chromatography/mass spectrometry (Trace MS equipped with a RTX-5 capillary column (30 m long $\times$ 0.25 mm internal diameter) and high purity nitrogen as carrier gas. The oven was programmed between 80 and 250°C at a heating temperature of 10°C min^{-1}. The GC retention data of the inhibitor corresponded to structural assignations performed at the National Institute of Standards and Technology (Gaithersburg, MD, USA) library search with a database and by mass spectra interpretation.

Inhibitor efficiency test

The rotating cage method. Corrosion inhibition efficiency was studied by the rotating cage test (ASTM G170; Papavinasam et al. 2000). API 5LX grade steel (C-0.29 max, S-0.05 max, P-0.04 max, Mn-1.25 max, remaining Fe) coupons of size 2.5 $\times$ 2.5 $\times$ 0.5 cm were mechanically polished to mirror finish and then degreased using trichloroethylene. Four coupons supported by polytetrafluoroethylene (PTFE) disks were mounted 55 mm apart on the

rotatory rod. Holes were drilled in the top and bottom PTFE plates of the cage to increase the turbulence on the inside surface of the coupon. The rod rotated at 200 rpm, which corresponded to a linear velocity of 0.53 m s^{-1}. In the present study, 500 ml of diesel with 2% water containing 120 ppm chloride as System I (control); 500 ml of diesel with 2% water containing 120 ppm chloride and 2 ml of mixed cultures of ACE2 and ACE4 as System II; 500 ml of diesel with 2% water containing 120 ppm chloride and 100 ppm of OSCI as System III; while 500 ml diesel with 2% of water containing 120 ppm chloride, 100 ppm of OSCI with 2 ml of mixed cultures of ACE2 and ACE4 as System IV. The concentration of cells in the inoculum was 2.14×10^8 CFU ml^{-1}.

The flow loop test-for simulating the stratification of water in pipe flow. The flow loop model was made in the laboratory for creating stagnant water in the pipeline for simulating the field conditions (Muthukumar et al. 2006). The flow loop system consisted of a reservoir that maintained the solution under test, a pump with piping and a by pass valve that controls the solution flow. The low velocity region was maintained in the cylindrical PVC pipe having a length of 20 cm and diameter of 12 cm. The suction line preceded the cylindrical device and the outlet from the device was connected to the reservoir. The experimental set-up was washed with distilled water and dried. Polished metal coupons were suspended in the setup in the hook provided. In the present study, the following systems were made: 8000 ml diesel + 2% water (120 ppm chloride) as System V (control); 8000 ml of diesel with 2% water containing 120 ppm chloride and 2 ml of mixed cultures of ACE2 and ACE4 as System VI; 8000 ml of diesel with 2% water containing 120 ppm chloride and 100 ppm of OSCI as System VII and 8000 ml diesel with 2% water containing 120 ppm chloride, 100 ppm of OSCI inoculated with 2 ml of mixed cultures of ACE2 and ACE4 as System VIII.

After 7 d, the coupons were removed and washed in Clark's Solution (Treseder et al. 1991) for 1 min to remove the corrosion products and rinsed with sterile distilled water and dried. The final weights of the six coupons in each system were taken and the average corrosion rates were also calculated and standard deviations are also presented. The inhibition efficiency (IE) was calculated as follows:

$$\text{Inhibition efficiency (IE \%)} = \frac{W - W_{inh}}{W} \times 100$$

where W_{inh} and W are the values of the weight-loss of steel after immersion in solutions with and without inhibitor, respectively.

Electrochemical method for the evaluation of inhibitor

After the weight loss experiments (rotating test), an impedance study was carried out in a cell containing aqueous medium collected from the rotating cage and flow loop methods (Schiapparelli & Meybaum, 1980; Rajasekar et al. 2006). API 5LX steel coupon of size 1 cm^2 as a working electrode, a standard calomel electrode (SCE) and platinum wire as counter electrode were employed for impedance studies. An EG & G electrochemical impedance analyser (Model M6310 with software M398) was used for AC impedance measurements. After attainment of a steady state potential an AC signal of 10 mV amplitude was applied and impedance values were measured for frequencies ranging from 100 kHz to 0.01 Hz. The values of charge transfer resistance (R_{ct}) were obtained from the Bode plots.

Surface analytical study

The surface morphological characteristics of the control and experimental carbon steel were imaged with a scanning electron microscope (SEM) Hitachi model S-3000H at magnifications ranging from 50X to 500X operated at an accelerating voltage of 25 kV.

Results and discussion

Biodegradation analysis

Growth of bacteria. The bacterial population ranged between 10^5 and 10^9 CFU ml^{-1} in the presence of the OSCI. In the absence of the OSCI, the total bacterial count (ACE2 and ACE4) decreased from 2.2×10^6 to 6.5×10^5 CFU ml^{-1} although the initial inoculum (2.14×10^8 CFU ml^{-1}) was same in all the systems. The proliferation of bacteria was higher in the presence of the OSCI compared with the absence of the inhibitor. It could be explained by the fact that that ACE2 and ACE4 utilise the inhibitor as an organic source with inorganic nutrients from the BH media for their proliferation. It indicates that the OSCI enhanced the proliferation of the bacteria ACE2 and ACE4.

Degradation of the OSCI

The FTIR spectrum of the OSCI shows (Figure 1a) the presence of the methyl (CH_3) and methylene (CH_2) aliphatic saturated C-H stretching band at 2922 cm^{-1} and 2853 cm^{-1}, respectively. The C = O stretching band was observed at 1707 cm^{-1} due to the presence of carboxylic acid group in the OSCI. The peaks at 1459 and 1413 cm^{-1} were due to the aromatic C-C stretching band. The C-N asymmetric

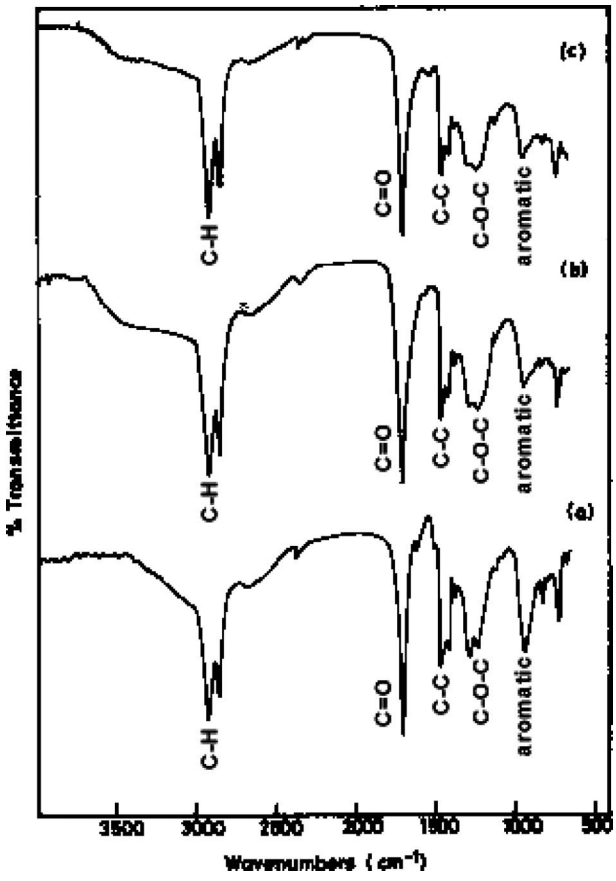

Figure 1. Fourier-transform infrared spectra. (a) OSCI (uninoculated system – control); (b) inoculated with *S. marcescens* ACE2; (c) inoculated with *B. cereus* ACE4.

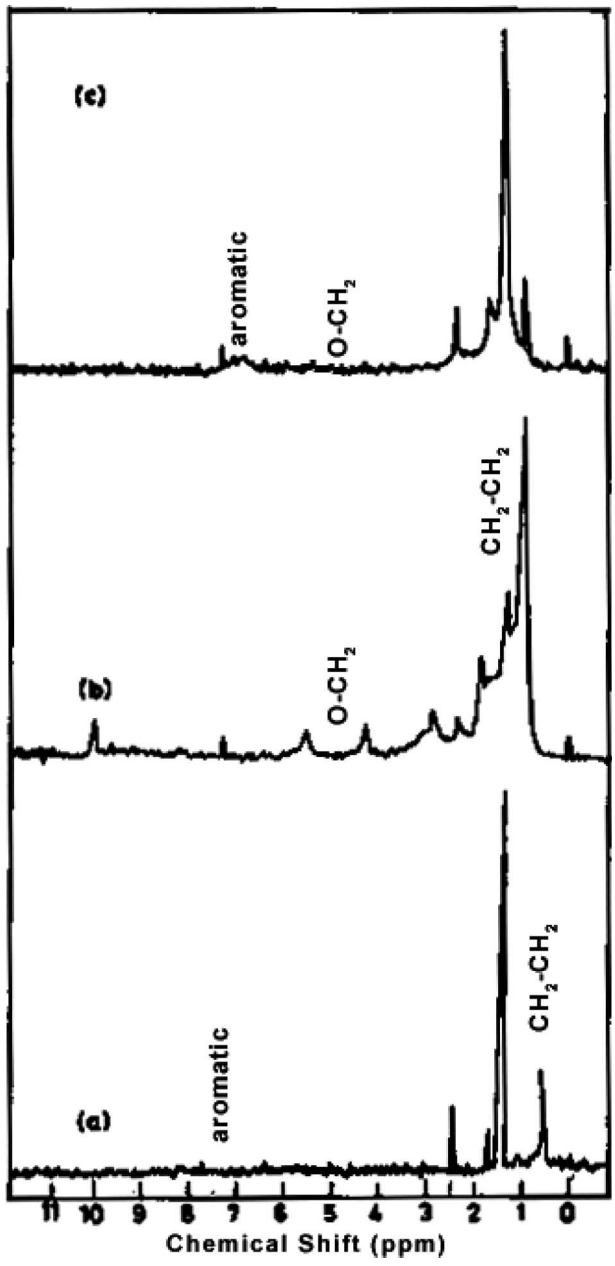

Figure 2. H^1 NMR Spectra. (a) OSCI (uninoculated system – control); (b) inoculated with *S. marcescens* ACE2; (c) inoculated with *B. cereus* ACE4.

stretching was observed at 1374 cm^{-1}. The peak at 1283 cm^{-1} was due to an aromatic C–O-C delocalisation band. The peak at 934 cm^{-1} was due to the substituted benzene ring. The aromatic bending band occurred at the range of 813 – 723 cm^{-1}.

The FTIR spectra of the OSCI with bacterial (ACE2 and ACE4) are presented in Figure 1b and 1c. A new peak was observed at 1237 cm^{-1} which indicates the carboxyl group. It can be assumed that oxygen addition takes place in presence of bacteria and the lesser intensity of the peak at 813 cm^{-1} indicates the consumption of aromatic moieties by bacterial activity.

The NMR spectrum of the OSCI is presented in Figure 2a. The aromatic proton peak was observed at 7 ppm as a singlet peak. The amine protons were observed at 3 ppm, 2.79 ppm and 2.29 – 1.9 ppm; the aliphatic methylene (CH_2) protons peaks at 1.59 and 1.29 ppm and methyl proton (CH_3) peak at 0.87 ppm. In the NMR spectrum of ACE2 inoculated OSCI (Figure 2b), the singlet peak at 6.1 ppm was attributed to olefinic protons, formed from the decomposition of aromatic ring and the olefinic proton peaks. A new peak was observed at 4.21 ppm, indicative of oxygen-bound protons (O-CH_2). The NMR data suggest that the ACE2 degraded or consumed the aliphatic hydrocarbon.

The NMR spectrum of the OSCI in the presence of ACE4 is presented in Figure 2c. The aromatic proton peak was observed at 7 ppm as a singlet peak. The amine proton peaks were observed at 2.82 ppm and in the range between 2.02 and 2.19. The aliphatic methylene proton peaks were observed at 1.5 and 1.28 and the methyl proton peak was observed at 0.91 ppm. The intensity of aliphatic proton peaks at (1.5, 1.28 and 0.91) was lesser in ACE2 when compared to ACE4 indicating that ACE2 consumed larger quantities of hydrogen

during the 30 d incubation. Both NMR and FTIR data indicate that ACE2 consumes both aliphatic and aromatic hydrocarbons present in the inhibitor while ACE4 consumes only aliphatic protons.

The GC retention data of the OSCI, OSCI with *S. marcescens* ACE2 and OSCI with *B. cereus* ACE4 are presented in Table I. The corrosion inhibitor (uninoculated system) consisted (Figure 3a) of aliphatic hydrocarbons including 2-docene-1-yl(-) succinic anhydride, bis (2-ethylhexyl) phthalate [1,2-benzene dicarboxylic acidbis (2-ethylhexyl) ester]. These compounds were the major components in the OSCI and the molecular weight was in the range 266 – 520.

In OSCI with ACE2 (Figure 3b), the aliphatic and aromatic components were not prominent and new peaks at 1.70, 3.79, 6.54, 7.42, 7.59, 8.38, 9.19, 9.94 min retention time indicated new compounds which were benzene,1-methyl-2-(1-methylethyl), naphthalene,2-methyl, benzene,1,1′-ethylidenebis, benzene,1,1′-methylenebis[4-methyl, benzene,1,1′-methylenebis[4-methyl, 3,5,3′,5′-tetramethyl biphenyl, 1,5,6,7-tetramethyl-3-phenylbicyclo [3,2,0] shepta-2,6-diene respectively. This is due to the decomposition or degradation of aromatic compounds. The present findings suggest that the strain ACE2 degraded both aliphatic and aromatic components and the molecular weight was reduced to between 142 and 224.

In OSCI with ACE4 along with OSCI (Figure 3c), the presence of new peaks indicate the new compounds benzene,1,1′-methylenebis[4-methyl, naphthalene,2-methyl, 1,1′-biphenyl,2-methyl, benzene, 1,1′,1″,1‴[1.6-hexadiylidene]-tetrakis, benzene1,5,6, 7-tetramethyl-3-phenylbicyclo[3,2,0]hepta-2,6-diene, benzene,1,1′-methylenebis[4-methyl, benzene,1,1′-methylenebis[4-methyl, 3,5,3′,5′-tetramethyl biphenyl, 1,5,6,7-tetramethyl-3-phenylbicyclo[3,2,0]hepta-2,6-diene,1,5,6,7-tetramethyl-3-phenylbicyclo[3,2,0] hepta-2,6-diene,1,5,6,7-tetramethyl-3-phenylbicyclo [3,2,0]hepta-2,6-diene and dibutylthalate. The chemical changes in the OSCI are due to the decomposition or degradation of aromatic compounds. The present finding suggests that the strain ACE4 has a high preference for degrading both aliphatic and aromatic components and the molecular weight is reduced to between 142 and 278.

The present study reveals that the isolates have the capacity to degrade both the aromatic and aliphatic hydrocarbon in the OSCI in a petroleum product pipeline which supports the observation made by Muthukumar et al. (2006) and Rajasekar et al. (2006) and where the water soluble inhibitor was degraded in the storage tank and transporting pipeline.

Table I. GCMS data for the OSCI, OSCI with *S. marcescens* ACE2 and OSCI with *B. cereus* ACE4.

Retention time (min)	Compound	Molecular formulae	Molecular weight	System
1.69	Benzene,1,1′-methylenebis[4-methyl-	$C_{15}H_{16}$	196	ACE4
1.70	Benzene,1-methyl-2-(1-methylethyl)	$C_{10}H_{14}$	224	ACE2
3.79	Naphthalene,2-methyl-	$C_{11}H_{10}$	142	ACE2, ACE4
5.39	1,1′-biphenyl,2-methyl-	$C_{13}H_{12}$	168	ACE4
6.31	Benzene,1,1′,1″,1‴[1.6-hexadiylidene]-tetrakis- {Hexane 1,1,6,6-tetraphenyl}	$C_{30}H_{30}$	390	ACE4
6.54	Benzene,1,1′-ethylidenebis- {Ethane 1,1-diphenyl}	$C_{14}H_{14}$	182	ACE2
6.55	Benzene 1,5,6,7-tetramethyl-3-phenylbicyclo[3,2,0]hepta-2,6-diene	$C_{17}H_{20}$	224	ACE4
7.42	Benzene,1,1′-methylenebis[4-methyl-	$C_{15}H_{16}$	196	ACE2, ACE4
7.59	Benzene,1,1′-methylenebis[4-methyl-	$C_{15}H_{16}$	196	ACE2, ACE4
8.38	3,5,3′,5′-tetramethyl biphenyl	$C_{16}H_{18}$	210	ACE2, ACE4
9.05	2-Docene-1-yl(-) succinic anhydride	$C_{16}H_{26}O_3$	266	OSCI
9.19	1,5,6,7-tetramethyl-3-phenylbicyclo[3,2,0]hepta-2,6-diene	$C_{17}H_{20}$	224	ACE2, ACE4
9.56	2-Docene-1-yl(-) succinic anhydride	$C_{16}H_{26}O_3$	266	OSCI
9.86	2-Docene-1-yl(-) succinic anhydride	$C_{16}H_{26}O_3$	266	OSCI
9.94	1,5,6,7-tetramethyl-3-phenylbicyclo[3,2,0]hepta-2,6-diene	$C_{17}H_{20}$	224	ACE2, ACE4
10.15	2-Docene-1-yl(-) succinic anhydride	$C_{16}H_{26}O_3$	266	OSCI
10.29	1,5,6,7-tetramethyl-3-phenylbicyclo[3,2,0]hepta-2,6-diene	$C_{17}H_{20}$	224	ACE4
10.32	2-Docene-1-yl(-) succinic anhydride	$C_{16}H_{26}O_3$	266	OSCI
10.82	2-Docene-1-yl(-) succinic anhydride	$C_{16}H_{26}O_3$	266	OSCI
11.10	Dibutylthalate	$C_{16}H_{22}O_4$	278	ACE4
11.14	2-Docene-1-yl(-) succinic anhydride	$C_{16}H_{26}O_3$	266	OSCI
12.94	2-Docene-1-yl(-) succinic anhydride	$C_{16}H_{26}O_3$	266	OSCI
16.22	Bis (2-ethylhexyl) phthalate [1,2-Benzene dicarboxylic acid bis (2-ethylhexyl) ester]	$C_{27}H_{36}O_{10}$	520	OSCI

OSCI = oil soluble corrosion inhibitor; ACE2 = OSCI with *S. marcescens* ACE2; ACE4 = OSCI with *B. cereus* ACE4.

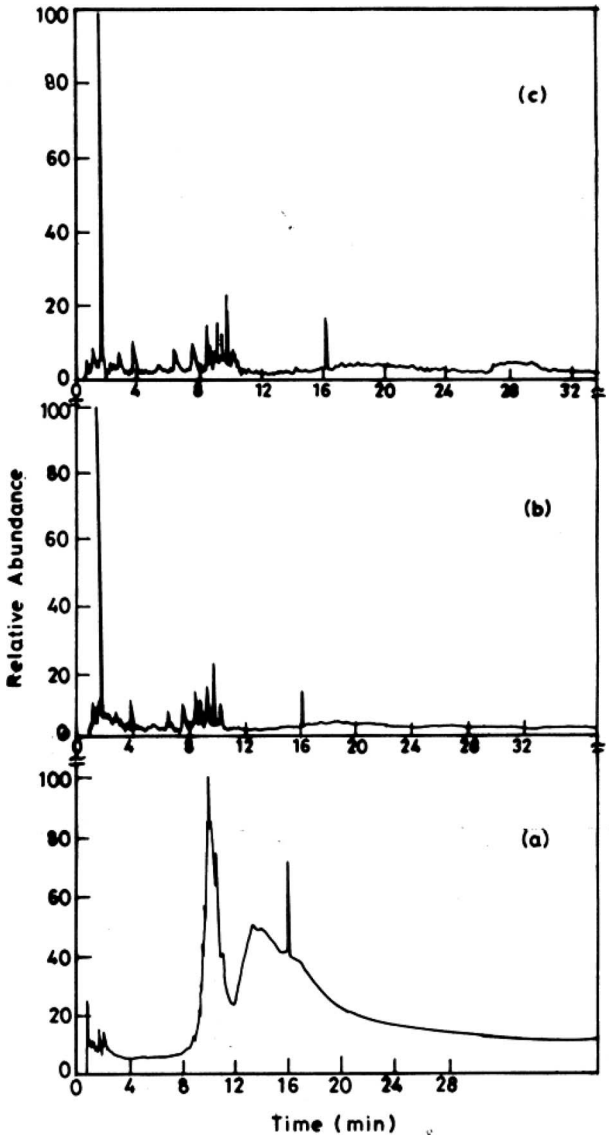

Figure 3. GC-MS spectra of (a) OSCI; (b) OSCI inoculated with ACE2; and (c) OSCI inoculated with ACE4.

Inhibitor efficiency

The rotating cage method. The inhibition efficiency (IE) of the OSCI derived by the rotating cage method is presented in Table II. The corrosion rate of API 5LX in a control system (without inoculum) was 0.3.3 mm year^{-1} after 168 h. In the presence of bacteria without a corrosion inhibitor (System II), the corrosion rate increased to (0.51 mm year^{-1}). The inhibition efficiency of the OSCI decreased from 62% to 29% due to the presence and activities of the bacteria. This observation indicated that bacteria reduced the efficiency of the OSCI.

The flow loop method. The inhibition efficiency (IE) of the OSCI determined by the flow loop method is presented in Table II. The corrosion rate of API 5LX in a control system (System V, without inoculum) was 0.04 mm year^{-1} after 168 h. In the presence of bacteria and no CI (System VI), the corrosion rate was higher 0.09 mm year^{-1} when compared to the absence of microbes. The OSCI gave an inhibition efficiency of 31% (System VII) while in presence of the OSCI along with bacteria; the inhibition efficiency was -27% (System VIII). This observation supported the conclusion that the bacteria reduced the efficiency of the OSCI.

Electrochemical study

The charge transfer resistance (R_{ct}) and double layer capacitance (C_{dl}) values were derived from the impedance measurements and presented in the Table III and Figure 4. The charge transfer resistance (R_{ct}) values for the control system and the bacterial system were in the range 1.02×10^4 ohm cm^{-2} to 5.77×10^3 ohms cm^{-2}. In the presence of the OSCI and inhibitor with mixed cultures (ACE2 and ACE4), the R_{ct} values were 1.68×10^6 ohm cm^{-2} and 4.56×10^6 ohm cm^{-2}, respectively. It also indicated that although the bacteria encouraged corrosion significantly, the OSCI gave better efficiency against 2% water and bacteria. Impedance data support the weight loss results. Addition of the OSCI decreased the double layer capacitance (C_{dl}) value from 5.24×10^{-7} F cm^{-2} corresponding to the control (System I) value. Decreases in the C_{dl} values were due to the decrease in the local dielectric constant and/or an increase in the thickness of the electrical double layer by the adsorption of the OSCI at the metal-solution interface (Caffeer & Hackerman, 1972). However, the OSCI alone showed a decrease in C_{dl} values by three orders of magnitude. In the presence of bacteria (ACE 2 and ACE 4) along with the OSCI an increase in C_{dl} values by one order was observed when compared to the inhibitor addition System III.

The charge transfer resistance (R_{ct}) and double layer capacitance (C_{dl}) values were derived from the impedance measurements and are presented in the Table III and Figure 5. The charge transfer resistance (R_{ct}) values for the control system and the bacterial system were in the range 3.19×10^4 ohm cm^{-2} to 2.75×10^4 ohms cm^{-2}. In the presence of the OSCI and inhibitor with mixed cultures (System VIII), the R_{ct} values were 3.95×10^4 ohm cm^{-2} and 7.38×10^3 ohm cm^{-2}, respectively. The R_{ct} value of the OSCI was higher when compared to inhibitor with bacterial cultures. This could be explained by the fact that due to the degradation of inhibitor the efficiency decreased. Or it may be due to the bacteria degrading the OSCI in the diesel-water system. The addition of the OSCI decreased the double layer

Table II. Corrosion rates of API 5LX with OSCI in the rotating cage system and the flow loop method.

Sl. no	System	Weight loss (mg)	Corrosion rate (mmpy)	Inhibition efficiency (%)
	Rotating cage system			
1	*System I*: 500 ml of diesel + 5% water (containing 120 ppm chloride)	26.5	0.3262	–
2	*System II*: 500 ml of diesel + 5% water (containing 120 ppm chloride) + bacterial culture	41.7	0.5133	–
3	*System III*: 500 ml of diesel + 2% water (containing 120 ppm chloride) + OSCI (100 ppm)	10	0.1230	62
4	*System IV*: 500 ml of diesel + 5% water (containing 120 ppm chloride) + bacterial culture + OSCI (100 ppm)	30	0.3690	29
	Flow loop method			
5	*System V*: 8000 ml of diesel + 2% water (containing 120 ppm chloride)	7.56	0.0440	–
6	*System VI*: 8000 ml of diesel + 2% water (containing 120 ppm chloride) + bacterial culture	15.3	0.0891	–
7	*System VII*: 8000 ml of diesel + 2% water (containing 120 ppm chloride) + OSCI (100 ppm)	5.2	0.0303	31
8	*System VIII*: 8000 ml of diesel + 2% water (containing 120 ppm chloride) + bacterial culture + OSCI (100 ppm)	9.6	0.0558	−27

Table III. Impedance data for the OSCI in the rotating cage system and flow loop method.

Sl. no	System	R_{ct} (ohm cm^{-2})	C_{dl} (F cm^{-2})
	Rotating cage system		
1	*System I*: (control): diesel + 2% water	1.02×10^4	5.24×10^{-7}
2	*System II*: diesel + 2% water + 2 ml mixed cultures (ACE2 and ACE4)	5.77×10^3	1.51×10^{-8}
3	*System III*: diesel + 2% water + OSCI (100 ppm)	1.68×10^6	5.25×10^{-10}
4	*System IV*: diesel + 2% water + 2 ml mixed cultures (ACE2 and ACE4) + OSCI (100 ppm)	4.56×10^6	6.80×10^{-9}
	Flow loop method		
5	*System V*: 8000 ml of diesel + 2% water (containing 120 ppm chloride)	3.19×10^4	6.89×10^{-9}
6	*System VI*: 8000 ml of diesel + 2% water (containing 120 ppm chloride) + bacterial culture	2.75×10^4	3.67×10^{-7}
7	*System VII*: 8000 ml of diesel + 2% water (containing 120 ppm chloride) + OSCI (100 ppm)	3.95×10^4	1.75×10^{-10}
8	*System VIII*: 8000 ml of diesel + 2% water (containing 120 ppm chloride) + bacterial culture + OSCI (100 ppm)	7.38×10^3	7.77×10^{-6}

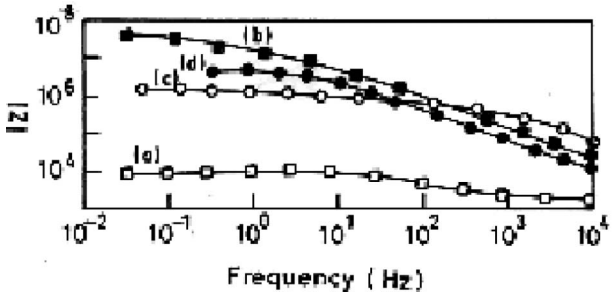

Figure 4. Bode plot for API 5LX in diesel water system in the presence and absence of OSCI in the rotating cage system. a = 500 ml diesel + 2% water; b = 500 ml diesel + 2% water + 2 ml mixed cultures (ACE2 and ACE4); c = 500 ml diesel + 2% water + OSCI (100 ppm); d = 500 ml diesel + 2% water + OSCI (100 ppm) + 2 ml mixed cultures (ACE2 and ACE4).

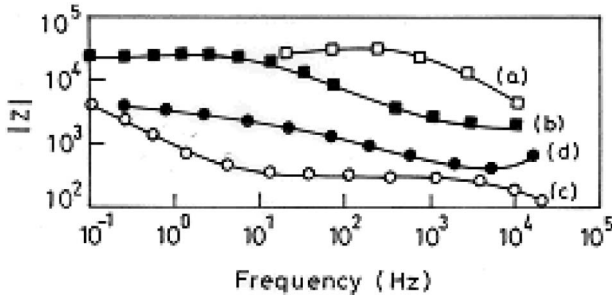

Figure 5. Bode plot for API 5LX in diesel water system in the presence and absence of OSCI in the flow loop system. a = 500 ml diesel + 2% water; b = 500 ml diesel + 2% water + 2 ml mixed cultures (ACE2 and ACE4); c = 500 ml diesel + 2% water + OSCI (100 ppm); d = 500 ml diesel + 2% water + OSCI (100 ppm) + 2 ml mixed cultures (ACE2 and ACE4).

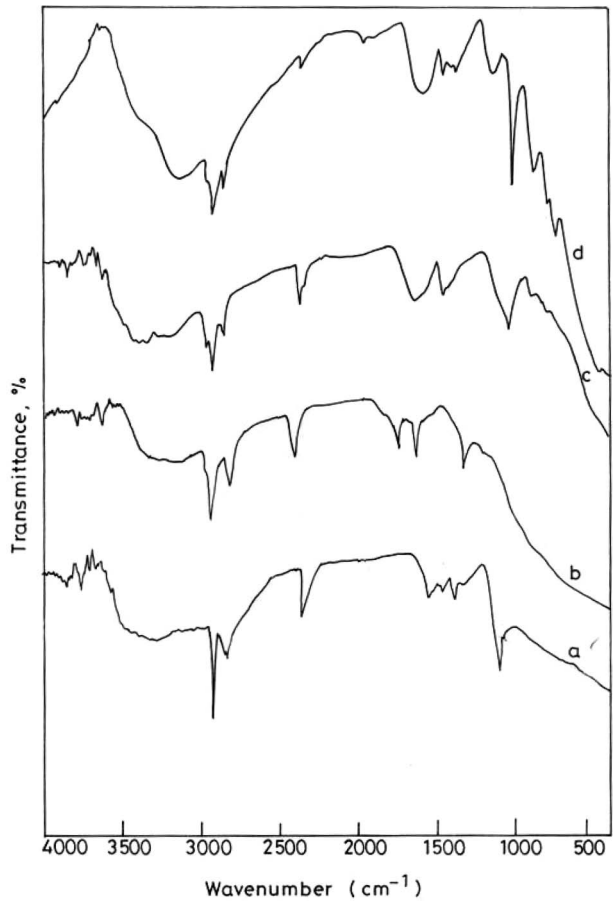

Figure 6. FTIR spectra for surface film collected in the rotating cage method. (a) System I; (b) System II; (c) System III, and (d) System IV.

capacitance (C_{dl}) value from 6.89×10^{-9} F cm^{-2} corresponding to the control (System V) value.

Surface analysis

FTIR studies in the rotating cage system. Figure 6a shows the FTIR spectrum of a corrosion product sample collected from the rotating cage system without inhibitor (System I). The peak at 3133 cm^{-1} indicates the presence of OH stretch. The peaks at 2922 cm^{-1} and 2852 cm^{-1} indicate the presence of CH aliphatic stretch. The peaks at 1576 cm^{-1} and 1457 cm^{-1} indicate the C=C aromatic nuclei. The peak at 1378 cm^{-1} indicates the presence of CH deformation for methyl group. The peaks at 1124 cm^{-1} and 1019 cm^{-1} indicate the C=O (carbonyl group) stretch for C-O-C group. It may be an ester peak. The peaks at 880 cm^{-1} and 745 cm^{-1} indicate the presence of substituted benzene peak. Figure 6b shows the FTIR spectrum of a sediment sample collected from the rotating cage system with bacterial culture (System II). A new peak at 1725 cm^{-1} indicates the presence of C=O (carbonyl group). Another peak at 1631 cm^{-1} indicates C=C conjugated diene and the peaks at 1461 cm^{-1} and

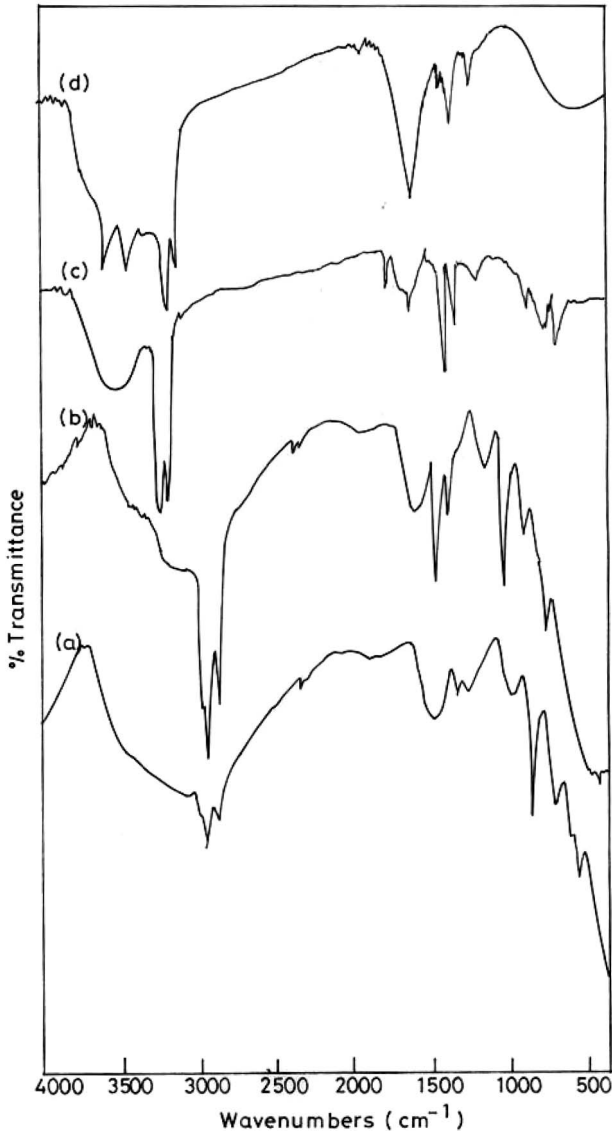

Figure 7. FTIR spectra for surface film collected by the flow loop method. (a) System V (Control); (b) System VI; (c) System VII (with inhibitor); and (d) System VIII.

1376 cm^{-1} indicate the CH def for methyl group. Figure 6c shows the FTIR spectrum of sediment sample collected from the rotating cage system with OSCI (System III). In this system a new peak was noticed at 1596 cm^{-1}, indicating the presence of carboxylate anion (COO^-) on the metal surface. It reveals that the added inhibitor contains mono carboxylic acid. Figure 6d shows the FTIR spectrum of sediment sample collected from the rotating cage system in the presence of inhibitor with bacterial culture (System IV). The new peaks at 1805 cm^{-1}, 1776 cm^{-1} and 1754 cm^{-1} indicate the presence of C=O group. A peak at 1632 cm^{-1} indicates the presence of conjugated diene.

FTIR studies in flow loop system. The FTIR spectrum of corrosion product collected from flow loop

system without inhibitor (System V) is presented in Figure 7a. The peaks identified in the control system (System V) are similar to the peaks noticed in System I. Figure 7b shows the FTIR spectrum of a sediment sample collected from the flow loop system with bacterial culture (System VI). In System VI, the same number of peaks as in System V was noticed.

The commercially available OSCI, Baker NC 351, consisted of amine based carboxylic acid compounds. While adding the inhibitor in the flow loop method (Figure 7c, 7d), both the components adsorbed on the metal surface and inhibited corrosion. The peak at 3425 cm^{-1} and 3254 cm^{-1} indicate the presence of NH aliphatic stretch. The peaks at 2925 cm^{-1} and 2854 cm^{-1} indicate the presence of CH aliphatic stretch. The peaks at 1596 cm^{-1} and 1459 cm^{-1} indicate the presence of C = C aromatic nuclei. The peaks at 1375 cm^{-1} show the CH def for methyl group. The peaks at 1145 cm^{-1} and 1019 cm^{-1} indicate the C = O (carbonyl group) stretch for C-O-C group. The peaks at 877 cm^{-1} and 745 cm^{-1} indicate the presence of substituted benzene compounds. The peaks at 2925 cm^{-1} and 2855 cm^{-1} indicate the presence of a CH aliphatic group. A peak at 1633 cm^{-1} indicates a C = C conjugated diene. A peak at 1443 cm^{-1} indicates the CH def for methyl group. Another peak at 1020 cm^{-1} indicates the CO stretch for C-O-C group. It reveals that the added inhibitor contains amine-based carboxylic acid. But in the presence of inhibitor together with bacteria, the carbonyl group for acid group [C = O, 1710 cm^{-1}] could not be adsorbed on the metal surface. Besides, due to bacterial adhesion on the metal surface, the carbonyl group of the acid group (C = O) to carboxylate anion group (COO^-) were noticed. Hence, the efficiency of the inhibitor was reduced about 33% in the rotating cage method and 58% in the flow loop method. The present observation supports the observations of Rajasekar et al. (2006).

Surface analysis

SEM analysis

SEM micrographs of the metal surface were recorded before and after treatment with inhibitor (Figure 8a – 8d). In the absence of inhibitor (Figure 8a) the pitting type of corrosion was observed whereas in presence of the inhibitor

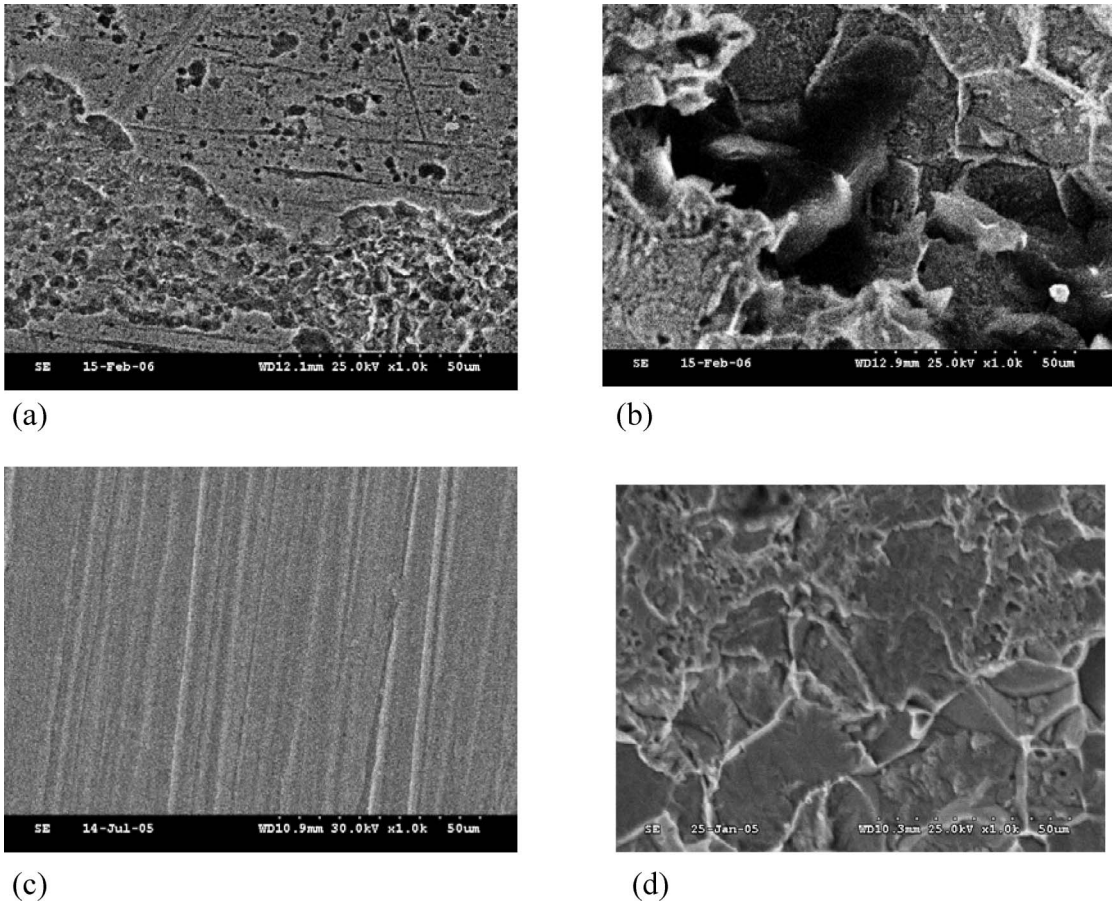

Figure 8. SEM images of API 5LX in the presence and absence of inhibitor in the rotating cage system. (a) System I; (b) System II; (c) System III; and (d) System VI.

(OSCI) there was only very mild uniform corrosion (Figure 8c). Pitting type corrosion was observed both in the presence of bacterial cultures alone and with the inhibitor system (Figure 8b – 8d).

Conclusions

i) The FTIR, NMR and GCMS results reveal that *S. marcescens* ACE2 is a major aliphatic and aromatic hydrocarbon degrader when compared to *B. cereus* ACE4; ii) the weight loss data and impedance study reveal that bacterial cultures may reduce the efficiency of the inhibitor. This is due to the degradation of the inhibitor in the system. The reduction in efficiency of the inhibitor was higher in the flow loop method than in the rotating cage method, indicating that the water stagnation point in the flow system may enhance inhibitor degradation, which may affect inhibition efficiency; and iii) the present study reveals that non-degradable OSCI may be needed for petroleum product pipelines to avoid microbial degradation of the corrosion inhibitor.

Acknowledgements

The authors wish to express their thanks to the Director, CECRI, Karaikudi-6 for his kind permission to publish these results. One of the authors, N. Muthukumar, thanks CSIR for the award of a Senior Research Fellowship. The authors also thank Mr A. Rajasekar, SRF and Prof. S. Karuthapandian, Head of the Biotechnology Department, Alagappa University, Karaikudi for providing the identified bacterial species and are grateful to Dr S. Sathiyanarayanan for his kind help with the electrochemical techniques.

References

Bento FM, Gaylarde CC. 2001. Biodeterioration of stored diesel oil: studies in Brazil. Int Biodeterior Biodegr 47:107 – 112.

Bento FM, Beech IB, Gaylarde CC, Englert GE, Muller IL. 2005. Degradation and corrosive activities of fungi in a diesel – mild steel – aqueous system. World J Microbiol Biotechnol 21:135 – 142.

Caffeer MC, Hackerman N. 1972. Double layer capacitance of iron and corrosion inhibition with polymethylene diamines. J Electrochem Soc 119:146 – 154.

Freiter ER. 1992. Effect of a corrosion inhibitor on bacteria and microbiologically influenced corrosion. Corrosion 48:266 – 276.

Jones DA, Amy PS. 2002. A thermodynamic interpretation of microbiologically influenced corrosion. Corrosion 58:638 – 645.

Lin LH, Michael GE, Kovachev G, Zhu H, Philip RP, Lewis CA. 1989. Biodegradation of tar-sand bitumens from the Ardmore and Anadarko Basins, Carter country, Oklahoma. Org Geochem 14:511 – 523.

Little B, Ray R. 2002. A perspective on corrosion inhibition by biofilms. Corrosion 58:424 – 428.

Maruthamuthu S, Mohanan S, Rajasekar A, Muthukumar N, Ponmarippan S, Subramanian P, Palaniswamy N. 2005. Role of corrosion inhibitor on bacterial corrosion in petroleum product pipelines. Ind J Chem Tech 12:267 – 275.

Muthukumar N, Maruthamuthu S, Palaniswamy N. 2006. Water soluble inhibitor on microbially influenced corrosion diesel transporting pipeline. Colloids Surf Biointerfaces B 53:260 – 270.

Muthukumar N, Mohanan S, Maruthamuthu S, Subramanian P, Palaniswamy N, Raghavan M. 2003. Role of *Brucella* sp. and *Gallionella* sp. in oil degradation and corrosion. Electrochem Comm 5:421 – 427.

Papavinasam S, Revie RW, Attard M, Demoz A, Sun H, Donini JC, Michaelian KH. 2000. Laboratory methodologies for corrosion inhibitor selection. Mater Perf 39:58 – 60.

Pope DH, Zintel TP, Cookingham BA, Morris RG, Howard D, Day RA, Frank JR, Pogemiller GE. 1989. Mitigation strategies for microbiologically influenced corrosion in gas industry facilities. CORROSION/89, Paper no.192. Houston, TX: NACE. pp 1 – 15.

Poupin P, Truffaut N, Combourieu B, Besse P, Sancelme M, Veschambre H, Delort AM. 1998. Degradation of morpholine by an environmental *Mycobacterium* strain involves a cytochrome P-450. Appl Environ Microbiol 64:159 – 165.

Prasad R. 1998. Selection of corrosion inhibitors to control microbiologically influenced corrosion, CORROSION/98, Paper no. 276. Houston, TX: NACE International. 12 p.

Rajasekar A, Maruthamuthu S, Palaniswamy N, Rajendran A. 2006. Biodegradation of corrosion inhibitors and their influence on petroleum product pipeline. Microbiol Res (In press).

Ram NM, Correll Morris J. 1982. Selective passage of hydrophilic nitrogenous organic materials through macro reticular resins. Environ Sci Technol 16:170 – 174.

Schiapparelli R, Meybaum E. 1980. Microbial contamination and corrosion of aircraft integral fuel storage tanks – evaluation and risk control. Mater Perf 19:41 – 44.

Shennan JL. 1988. Control of microbial contamination of fuels in storage. In: Houghton DR, Smith RN, Eggins HOW, editors. Biodeterioration. Vol 7. Barking, UK: Elsevier. pp 248 – 254.

Treseder RS, Baboian R, Munger CG. 1991. NACE Corrosion engineer's reference book. Houston, TX: NACE International. TIC 245834.

Videla HA, Characklis WG. 1992. Biofouling and microbially influenced corrosion. Int Biodeterior Biodegr 29:195 – 212.